RBRC-671
SLAC-PUB-12503

Effect of Orbital Angular Momentum on Valence-Quark Helicity Distributions

Harut Avakian,[1] Stanley J. Brodsky,[2] Alexandre Deur,[1] and Feng Yuan[3]

[1] *Thomas Jefferson National Accelerator Facility, Newport News, VA 23606*

[2] *Stanford Linear Accelerator Center, Stanford University, Stanford, CA 94309*

[3] *RIKEN/BNL Research Center, Building 510A, Brookhaven National Laboratory, Upton, NY 11973*

(Dated: February 1, 2008)

Abstract

We study the quark helicity distributions at large x in perturbative QCD, taking into account contributions from the valence Fock states of the nucleon which have nonzero orbital angular momentum. These states are necessary to have a nonzero anomalous magnetic moment. We find that the quark orbital angular momentum contributes a large logarithm to the negative helicity quark distributions in addition to its power behavior, scaling as $(1-x)^5 \log^2(1-x)$ in the limit of $x \to 1$. Our analysis shows that the ratio of the polarized over unpolarized down quark distributions, $\Delta d/d$, will still approach 1 in this limit. By comparing with the experimental data, we find that this ratio should cross zero at $x \approx 0.75$.

PACS numbers: 12.38.Bx, 12.39.St, 13.85.Qk

1. Introduction. Power-counting rules for the large-x parton distributions in hadrons have been derived more than three decades ago based on perturbative quantum chromodynamics (pQCD) combined with a S-wave quark model of hadrons [1, 2, 3, 4]. The basic argument is that when the valence quark carries nearly all of the longitudinal momentum of the hadron, the relevant QCD configurations in the hadronic wave function become far off-shell and can be treated in pQCD. A generic factorization has recently been used to justify the power-counting rule by relating the parton distributions at large-x to the quark distribution amplitudes of hadrons [5]. The power-counting rule has also been generalized to sea quarks, gluons, helicity-dependent distributions [6, 7], and generalized parton distributions [8].

The leading pQCD diagrams associated with the leading Fock state of the proton wave function predict that the positive helicity (quark spin aligned with the proton spin) quark distribution $q^+(x)$ scales as $(1-x)^3$, ($x = k^+/P^+$ is the light-cone momentum fraction of the struck quark and is identical to the Bjorken x_B in the leading twist approximation), whereas the negative helicity (quark spin anti-aligned with the proton spin) quark distribution $q^-(x)$ is suppressed by $(1-x)^2$ relative to the positive helicity one, scaling as $(1-x)^5$ at large x [3]. The direct consequence of these power laws for the quark distributions is that the ratio of polarized quark distribution $\Delta q(x) = q^+(x) - q^-(x)$ over the unpolarized quark distribution $q(x) = q^+(x) + q^-(x)$ approaches 1 in the limit $x \to 1$; i.e., at large x, q^+ dominates over q^-. When this prediction is compared to the experimental data [9, 10, 11, 12], it is interesting to observe that, for the up quark the ratio increases with x, and seems to approach 1 at large x. However, the ratio for the down quark is still far below 1, and remains negative for a wide range of $x < 0.6$ [9]. This discrepancy has stimulated much theoretical interest.

In this paper we will reexamine the large-x quark helicity distributions in the perturbative QCD framework [3, 4]. We work in light-cone gauge with $A^+ = 0$, where there is no ghost contributions, and orbital angular momentum is physical [13]. We will take into account the contributions from not only the leading light-cone Fock state expansion of the nucleon wave function with zero quark orbital angular momentum ($L_z = 0$), but also the valence Fock states with nonzero quark orbital angular momentum ($L_z \neq 0$). These contributions are naturally required to obtain a nonzero anomalous magnetic moment for nucleons [14] and are also present in the wave function solutions in the AdS/CFT correspondence approach [15]. We find that for the negative quark helicity distribution q^-, there exist large logarithmic

enhancements from the $|L_z| = 1$ Fock state component of the proton. With this large logarithmic modification, we can explain the discrepancy between the power-counting rule and experimental data.

2. Analysis of the large-x behavior of the quark helicity distributions. In the $x \to 1$ regime where the struck quark has nearly all of the light-cone momentum of its parent hadron, the relevant QCD dynamics becomes far-off the mass shell: the Feynman virtuality of the struck quark becomes highly space-like: $k_F^2 - m^2 \sim -\frac{k_\perp^2 + \mathcal{M}^2}{1-x}$, where $k_\perp$ is the transverse momentum of the struck quark and $\mathcal{M}$ is the invariant mass of the spectator system. Thus we can use perturbative QCD to analyze the large-x behavior of the parton distributions since the internal propagators in the relevant Feynman diagrams scale as $1/(1-x)$. This behavior leads to the power-counting rules. In fact, more partons in the hadron's wave function mean more propagators in the scattering amplitudes and more suppression for the contribution to the parton distributions. Thus the parton distributions at large-x depend on the number of spectator partons in the Fock state wave function of the hadron. For example, the valence quark distributions of nucleon will be dominated by the three-quark Fock states of the nucleon wave function. The three-quark Fock state expansion of the nucleon wave function consists of zero orbital angular momentum component ($L_z = 0$) and nonzero orbital angular momentum component ($L_z \neq 0$) [16]. In the following discussion, we will consider the contributions from both Fock state components.

In the original power-counting analysis of the quark helicity distributions [6], only the contributions from the leading Fock state with $L_z = 0$ have been taken into account. In Fig. 1(a,b) we show the typical diagrams which contribute to the positive (a) and negative (b) quark helicity distributions at large x. In terms of the leading order quark distribution amplitude which corresponds to the $L_z = 0$ Fock state expansion of the proton wave function [4], these quark helicity distributions can be written as,

$$q^{\pm}(x)|_{x\to 1} = \int [dy_i][dy_i'] \Phi(y_i) \Phi'(y_i') \mathcal{H}^{(\pm)}(y_i, y_i'; (1-x)) \ , \tag{1}$$

where the integration measure $[dy_i]$ is defined as $[dy_i] = dy_1 dy_2 dy_3 \delta(1 - y_1 - y_2 - y_3)$, and the y_i are the light-cone momentum fractions of the proton carried by the quarks in the light-front wave functions, i.e., $p_i = y_i P$ and $p_i' = y_i' P$ in Fig. 1. Here, Φ and Φ' represent the quark distribution amplitudes of the proton at the left and right sides of the cut line, respectively. $\mathcal{H}$ represents the hard part of the amplitude which depends on y_i and y_i', and

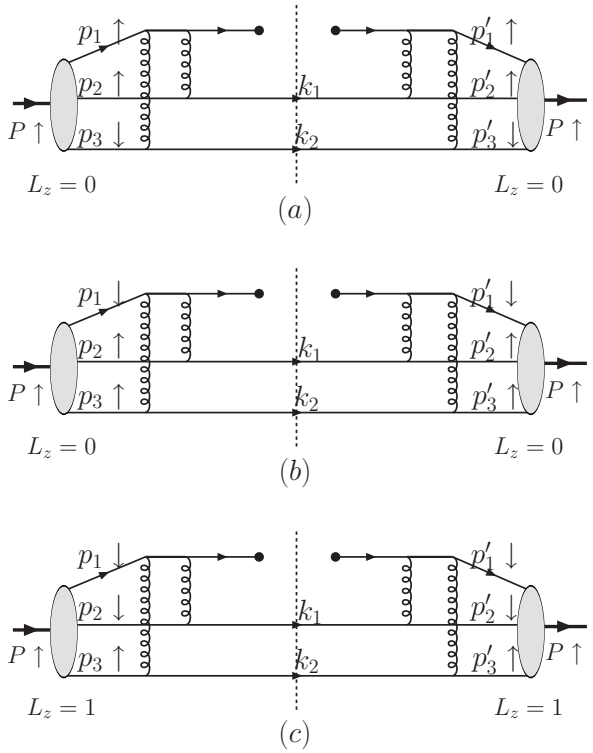

FIG. 1: *Examples of Feynman diagrams which contribute to the $q^{\pm}$ quark distributions at large x: (a) for q^+ with power contribution of $(1-x)^3$; (b) for q^- with $(1-x)^5$; (c) for q^- with $(1-x)^5 \log^2(1-x)$. The wave functions at the left and right sides of the cut line in (a) and (b) represent the leading Fock state expansion with zero quark orbital angular momentum, whereas those for (c) represent the valence Fock state with one-unit of quark orbital angular momentum.*

$(1-x)$ as well.

The large-x behavior of the hard factor $\mathcal{H}$ can be evaluated from the partonic scattering amplitudes as shown by the Feynman diagrams in Fig. 1. The wave functions corresponding to Figs. 1(a,b) have zero quark orbital angular momentum, and thus the total quark spin will be equal to the proton spin. If the struck quark spin is the same as the proton spin (for the positive helicity quark distribution q^+), the two spectator quarks will be in the spin-0 configuration, whereas for the negative helicity quark distribution q^- with the quark spin opposite to the proton spin, the two spectator quarks will be in the spin-1 configuration. It has been known for a long time that the hard partonic part $\mathcal{H}$ with a spin-1 configuration for the two spectators will be suppressed by $(1-x)^2$ relative to that with spin-0 configuration [3, 7, 17]. That is also the reason why the negative helicity quark distribution is suppressed

by $(1-x)^2$ relative to the positive helicity quark distribution from this contribution.

The far-off-shell propagators in the partonic Feynman diagrams are the dominant contributions to the power-counting of $(1-x)$ at large x. One of the gluon propagators in Fig. 1 behaves as

$$\frac{1}{(p_3-k_2)^2} = \frac{1}{2p_3\cdot k_2} \approx -\frac{1}{\langle k_\perp^2\rangle}\frac{1-x}{y_3} \ , \tag{2}$$

at large x. In the above expression, we have omitted all higher order terms suppressed by $(1-x)$. Here, $\langle k_\perp^2\rangle \sim \langle k_{1\perp}^2\rangle \sim \langle k_{2\perp}^2\rangle$, represents a typical transverse momentum scale for the spectator system. Each propagator will provide a suppression factor of $(1-x)$. Counting the hard propagators in Fig. 1(a), we find the total suppression factor from the hard propagators is

$$\sim \frac{(1-x)^8}{y_2y_3(1-y_2)y_2'y_3'(1-y_2')} \ . \tag{3}$$

We notice that the above expression does not introduce additional dependence on $(1-x)$ upon integration over y_i and y_i', assuming that the leading twist distribution amplitudes Φ and Φ' are proportional to $y_1y_2y_3$ and $y_1'y_2'y_3'$ [4], respectively. Combining these results with the power behavior for the other parts of the partonic scattering amplitudes and the phase space integral, we find the positive helicity quark distribution q^+ scales as $(1-x)^3$, whereas the negative helicity quark distribution q^- scales as $(1-x)^5$ [3, 4, 6, 7].

In the above analysis, we only considered the contributions from the leading Fock state of the proton with zero quark orbital angular momentum. In general, the contributions from the higher Fock states and the valence Fock states with nonzero quark orbital angular momentum will introduce additional suppression in (1-x) [4, 7]. However, the nonzero-quark-orbital-angular-momentum Fock state can provide large logarithmic enhancement to the helicity flip amplitudes. For example, it was found that the nonzero quark orbital angular momentum contributes a large logarithmic term to the nucleon's helicity-flip Pauli form factor $F_2(Q^2)$, which leads to the scaling behavior $F_2(Q^2) \sim \log^2(Q^2/\Lambda^2)/Q^6$ at $Q^2 \to \infty$ [18, 19]. This is consistent with recent experimental data from JLab [20]. In the following, we will study the nonzero quark orbital angular momentum contribution to the q^- quark distribution which is also associated with the helicity-flip amplitude. The corresponding contributions to the positive quark helicity distribution are always power suppressed [7].

In Fig. 1(c), we show an example of a contribution from the $L_z = 1$ Fock state of proton. Because the quark orbital angular momentum contributes one unit of the proton spin, we

can have difference between the total quark spin and the proton spin. If the two spectator quarks are in the spin-0 configuration, this will enhance the power-counting in the hard factor $\mathcal{H}$. On the other hand, in order to get a nonzero contribution, we have to perform the intrinsic transverse momentum expansion for the hard partonic scattering amplitudes [19], which will introduce an additional suppression factor in $(1-x)$ [7]. For example, one of the contributions from the diagram shown in Fig. 1(c) to the negative helicity quark distribution will be proportional to

$$q^-(x) \propto \int (p_1^x + ip_1^y)(p_1'^x - ip_1'^y)\tilde{\psi}^{(3)}(y_i, p_{i\perp})\tilde{\psi}^{(3)}(y_i', p_{i\perp}')T_H\left(y_i, p_{i\perp}; y_i', p_{i\perp}'\right) \ , \tag{4}$$

where $\tilde{\psi}^{(3)}$ is a light-front wave function amplitude for the $L_z = 1$ Fock state of the proton [16]. The intrinsic transverse momentum expansion is essential to get the nonzero contributions. Otherwise, the integral over the transverse momenta $p_{i\perp}$ and $p_{i\perp}'$ will vanish because of the explicit factors $p_1^x + ip_1^y$ and $p_1'^x + ip_1'^y$ in the above equation. One intrinsic transverse momentum expansion comes from the propagator we mentioned above,

$$\begin{aligned} \frac{1}{(p_3 - k_2)^2} &= \frac{1}{(y_3 P - k_2 + p_{3\perp})^2} \\ &\approx \frac{\beta(1-x)}{y_3 k_{2\perp}^2}\left(1 - \frac{\beta(1-x)}{y_3 k_{2\perp}^2} 2p_{3\perp}\cdot k_{2\perp}\right) \ , \end{aligned} \tag{5}$$

where β is defined as $k_2^+/(1-x)P^+$, and we have kept the linear dependence on $p_{3\perp}$ in the above expansion. Only this linear term will contribute when integrating over $p_{i\perp}$: $\int k_{2\perp} \cdot p_{3\perp}(p_1^x + ip_1^y)\tilde{\psi}^{(3)} \propto (k_2^x + ik_2^y)y_3\Phi_4(y_1, y_2, y_3)$, where Φ_4 is one of the twist-4 quark distribution amplitudes of the proton [19, 21]. From the above expansion, we find that this term will introduce additional factor of $(1-x)/y_3$ in the hard factor. Similarly, because of the $p_1'^x - ip_1'^y$ factor in Eq. (4), we have to do the expansion in intrinsic transverse momentum associated with the wave function at the right side of the cut line, and again the expansion of the gluon propagator with momentum of $p_3' - k_2$ will introduce another suppression factor of $(1-x)/y_3'$ in the hard factor. Thus the total suppression factor from the above two expansions will be $(1-x)^2/y_3 y_3'$, which gives the same power counting contribution to q^- as that from the leading Fock state with $L_z = 0$ in the above.

We thus find the contributions from $L_z = 1$ Fock state of the proton do not change the power counting for the q^- quark distribution at large x. However, the additional factor $1/y_3 y_3'$ from the intrinsic transverse momentum expansions will lead to a large logarithm

when integrating over y_i and y_i'. This is because, combining the above two factors with all other factors from the propagators shown in Eq. (3), the total dependence on y_i and y_i' for the hard factor will be

$$\sim \frac{1}{y_2 y_3^2 (1-y_2) y_2' y_3'^2 (1-y_2')} \ , \tag{6}$$

where we have y_3^2 and $y_3'^2$ in the denominator. On the other hand, we expect the twist-4 quark distribution amplitude to have the following behavior at the end point region: $y_3 \Phi_4(y_1, y_2, y_3) \propto y_1 y_2 y_3$ and $y_3' \Phi_4(y_1', y_2', y_3') \propto y_1' y_2' y_3'$ [21]. Thus we will have logarithmic divergences for the integrations over y_3 and y_3', for which we can regularize in terms of $\log(1-x)$ as indicated in the above propagator expansion. This will lead to a double logarithmic contribution $\log^2(1-x)$ in addition to the power term $(1-x)^5$ to the q^- quark distribution at large x.

In summary, for the negative quark helicity distribution q^- at large x, the leading Fock state with zero quark orbital angular momentum $L_z = 0$ contributes to a power term $(1-x)^5$, whereas the valence Fock state with $|L_z| = 1$ contributes to a double logarithmically enhanced term $(1-x)^5 \log^2(1-x)$. So, in the limit $x \to 1$, the q^- distribution will be dominated by the contributions from $L_z = 1$ Fock state of the proton, scaling as $(1-x)^5 \log^2(1-x)$. In the intermediate x range, the sub-leading terms can also be important. For example in Ref. [6], the quark helicity distributions were parameterized by the leading and sub-leading power terms and fit to the experimental data. This was later updated to account for the latest data in Ref. [22]. Thus, as a first step towards a comprehensive phenomenology, we follow the parameterizations for q^+ and q^- in Ref. [6] by adding the newly discovered double logarithms enhanced contributions,

$$\begin{aligned}
u^+(x) &= \frac{1}{x^\alpha} \left[A_u (1-x)^3 + B_u (1-x)^4 \right] \\
d^+(x) &= \frac{1}{x^\alpha} \left[A_d (1-x)^3 + B_d (1-x)^4 \right] \\
u^-(x) &= \frac{1}{x^\alpha} \left[C_u (1-x)^5 + C_u' (1-x)^5 \log^2(1-x) + D_u (1-x)^6 \right] \\
d^-(x) &= \frac{1}{x^\alpha} \left[C_d (1-x)^5 + C_d' (1-x)^5 \log^2(1-x) + D_d (1-x)^6 \right] \ ,
\end{aligned} \tag{7}$$

where the additional two parameters C_u' and C_d' come from the logarithmic modifications to the q^- quark distribution at large x, and all other parameters refer to [6]. In the following, we will fit to the current experimental data at large x region with the above parameterizations for the valence up and down quarks.

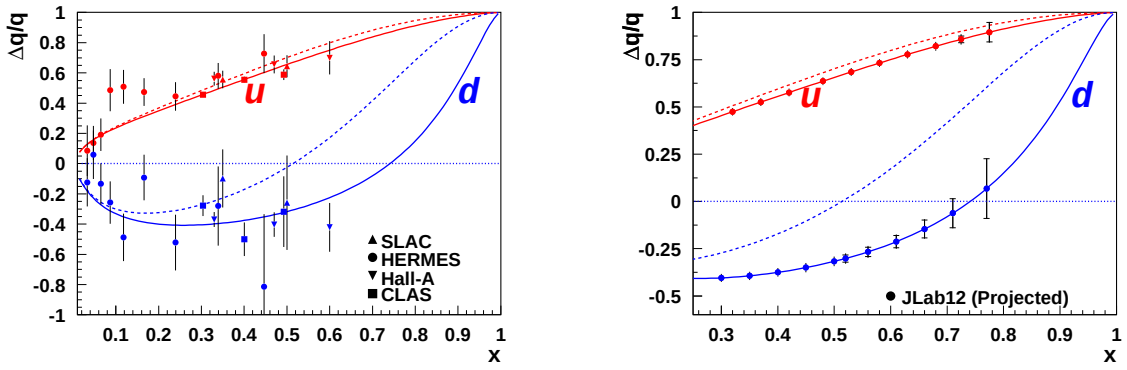

FIG. 2: *Comparison of the quark helicity distributions Eq. (7) with experimental data (left panel), and future projections from JLab (right panel) as functions of x for up (the upper curves) and down (the lower curves) quarks. The circles are for HERMES data [11], the triangles up for SLAC [12], the triangles down for JLab Hall-A data [9], the filled squares for CLAS [10], and open squares for 12 GeV upgrade projection for CLAS. The dashed curves are the predictions from [22], and the solid ones are our fit results (only the large-x (> 0.3) experimental data were used in the fit). The symbols in the right panel show combined projections from all three JLab experiments [24].*

3. Phenomenological applications. In order to demonstrate the importance of the new scaling behavior for the negative helicity distributions for the valence up and down quarks, we analyze the latest experimental data from SLAC, HERMES and Jefferson Lab, including Hall A and Hall B data [9, 10, 11, 12]. We will keep the original fit values for other parameters [22] except the two new parameters: C'_u and C'_d. We only use the experimental data in the large-x region, i.e., $x > 0.3$, where the sea contribution is not significant. We perform our fit at a fixed $Q^2 = 4$ GeV^2, and all the experimental data are evolved to this scale by using the GRSV parameterization [23] for the polarized and unpolarized quark distributions. The evolution introduces some theoretical uncertainties.

From our fit, we find the following values for C'_u and C'_d,

$$C'_u = 0.493 \pm 0.249, \qquad C'_d = 1.592 \pm 0.378 \ , \tag{8}$$

which are comparable in size to $C_u = 2.143 \pm 0.137$ and $C_d = 1.689 \pm 0.227$ in Ref. [22]. The minimum of the functional χ^2 is achieved at $\chi^2 = 11.4$ and $\chi^2/DOF = 11.4/10 = 1.14$. We further notice that the additional two terms in Eq. (7) do not change significantly the

sum rules for the up and down quarks, such as the Bjorken and momentum sum rule, which are essential for constraining the parameters in Refs. [6, 22]. For example, they contribute $\sim 4\%$ to the momentum sum rule coming from the quarks.

In the left panel of Fig. 2, we show the above fit, where we plot the ratio of the polarized quark distribution Δq over the unpolarized quark distributions q as functions of x for both up and down quarks, compared with the experimental data. From these comparisons, we find that the ratio for the up quark $\Delta u/u$ can still be described by the parameterization based on the original power counting rule for u^+ and u^-. This can also be seen from the small value of C'_u in our fit Eq. (8), with big error bar though. However, for the down quark we have to take into account a large contribution from the newly discovered term for the negative helicity distribution d^-; the difference between our result and the original power-counting-rule inspired parameterization [22] becomes significant at $x \gtrsim 0.5$. The analysis of the anomalous magnetic moment and generalized parton distributions of nucleons also indicates significant contributions from the orbital angular momenta of up and down quarks [25]. This is in qualitative agreement with our fitting results, taking into account the large error bar for C'_u. A precision determination of these contributions shall be obtained by further development for a consistent set of parameters for Eq. (7) from next-to-leading-order QCD analysis of both polarized and unpolarized data over the full range in x [22].

Another important prediction of our fit is that the ratio of $\Delta d/d$ will approach 1 at extremely large x, and it will cross zero at $x \approx 0.75$. It will be interesting to check this prediction in future experiments, such as the 12 GeV upgrade of Jefferson Lab. For comparison, in the right panel of Fig. 2, we show the experimental projections for these measurements from the 12 GeV upgrade of JLab experiments [24], together with our predictions and the results from the previous power-counting-rule parameterizations [22].

We thank N. Akopov, P. Bosted, J.P. Chen, V. Dharmawardane, Z.-D. Meziani and X. Zheng for useful conversations on the experimental data and many related discussions. We also thank X. Ji and W. Vogelsang for their comments. This work was supported by by the United States Department of Energy. Jefferson Science Associates (JSA) operates the Thomas Jefferson National Accelerator Facility for the U. S. DOE under contract DE-AC05-060R23177. F.Y. is grateful to RIKEN, Brookhaven National Laboratory and the U.S. DOE (grant number DE-FG02-87ER40371 and contract number DE-AC02-98CH10886) for

providing the facilities essential for the completion of this contribution.

---

[1] J. F. Gunion, Phys. Rev. D **10**, 242 (1974).

[2] R. Blankenbecler and S. J. Brodsky, Phys. Rev. D **10**, 2973 (1974).

[3] G. R. Farrar and D. R. Jackson, Phys. Rev. Lett. **35**, 1416 (1975).

[4] G. P. Lepage and S. J. Brodsky, Phys. Rev. D **22**, 2157 (1980).

[5] X. Ji, J. P. Ma and F. Yuan, Phys. Lett. B **610**, 247 (2005).

[6] S. J. Brodsky, M. Burkardt and I. Schmidt, Nucl. Phys. B **441**, 197 (1995).

[7] S. J. Brodsky and F. Yuan, Phys. Rev. D **74**, 094018 (2006).

[8] F. Yuan, Phys. Rev. D **69**, 051501 (2004).

[9] X. Zheng *et al.*, Phys. Rev. Lett. **92**, 012004 (2004); Phys. Rev. C **70**, 065207 (2004).

[10] K.V. Dharmawardane *et al.*, Phys. Lett. **B641**,11 (2006).

[11] A. Airapetian *et al.*, Phys. Rev. D **71**, 012003 (2005).

[12] K. Abe *et al.* [E154 Collaboration], Phys. Lett. B **405**, 180 (1997).

[13] S. J. Brodsky, H. C. Pauli and S. S. Pinsky, Phys. Rept. **301**, 299 (1998).

[14] S. J. Brodsky and S. D. Drell, Phys. Rev. D **22**, 2236 (1980).

[15] S. J. Brodsky and G. F. de Teramond, Phys. Rev. Lett. **96**, 201601 (2006).

[16] X. Ji, J. P. Ma and F. Yuan, Nucl. Phys. B **652**, 383 (2003).

[17] J. F. Gunion, P. Nason and R. Blankenbecler, Phys. Rev. D **29**, 2491 (1984).

[18] X. Ji, J. P. Ma and F. Yuan, Phys. Rev. Lett. **90**, 241601 (2003).

[19] A. V. Belitsky, X. Ji and F. Yuan, Phys. Rev. Lett. **91**, 092003 (2003).

[20] O. Gayou *et al.*, Phys. Rev. Lett. **88**, 092301 (2002).

[21] V. Braun, R. J. Fries, N. Mahnke and E. Stein, Nucl. Phys. B **589**, 381 (2000).

[22] E. Leader, A. V. Sidorov and D. B. Stamenov, Int. J. Mod. Phys. A **13**, 5573 (1998).

[23] M. Gluck, E. Reya, M. Stratmann and W. Vogelsang, Phys. Rev. D **63**, 094005 (2001).

[24] Jefferson Lab Hall A, B. Wojtsekhowski et al., JLab Proposal E12-06-122 (2006); Hall B, . S.Kuhn et al., E12-06-109 (2006); Hall C, X.Zheng et al., E12-06-110 (2006).

[25] M. Burkardt and G. Schnell, Phys. Rev. D **74**, 013002 (2006).